Chem

Photocatalytic hydrogenation of alkenes using ammonia-borane

Graphical abstract

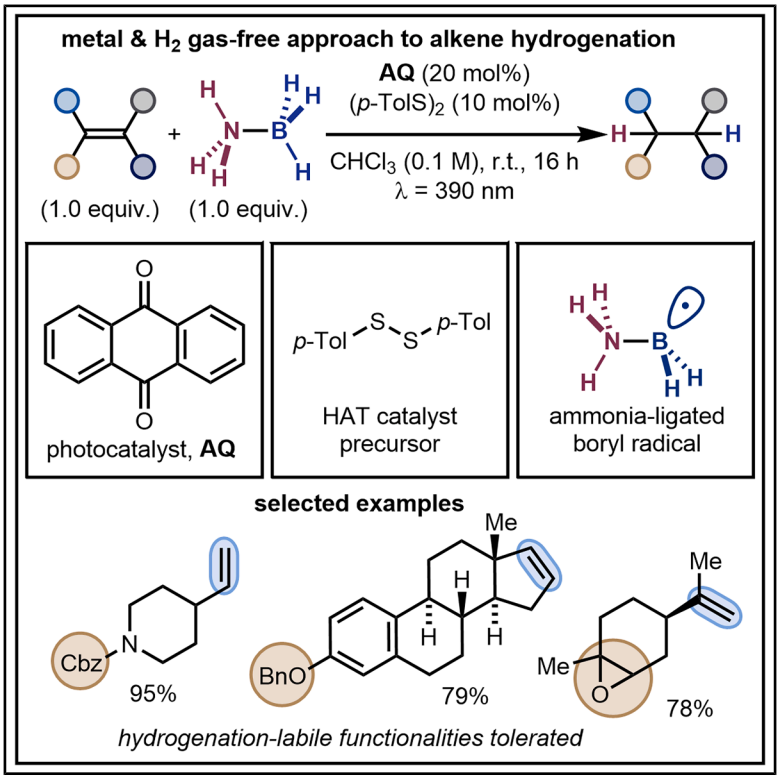

Highlights

- Photochemical activation of ammonia-borane enables hydrogenation of olefins
- Boryl radical intermediates are integral species in a complex mechanistic cascade
- Detailed mechanistic study through experimentation and computation

Authors

Eva Rivera-Chao, Wesley J. Olivier, Michael J. Tilby, Daniele Leonori

Correspondence

michael.tilby@bristol.ac.uk (M.J.T.), daniele.leonori@rwth-aachen.de (D.L.)

In brief

Hydrogenation of olefins is a key reaction in chemistry; however, it typically requires the use of flammable hydrogen gas with transition metal catalysis. This work presents a novel approach employing ammonia-borane, a stable and non-toxic reagent, as a hydrogen surrogate material under photocatalytic conditions, which efficiently circumvents the use of hydrogen and metal catalysis.

Rivera-Chao et al., 2026, Chem *12*, 102711
January 15, 2026
https://doi.org/10.1016/j.chempr.2025.102711

CellPress

Chem

CellPress
OPEN ACCESS

Article

Photocatalytic hydrogenation of alkenes using ammonia-borane

Eva Rivera-Chao,[1] Wesley J. Olivier,[1] Michael J. Tilby,[2,*] and Daniele Leonori[1,3,*]
[1]Institute of Organic Chemistry, RWTH Aachen University, Aachen 52056, Germany
[2]School of Chemistry, University of Bristol, Bristol BS8 1TS, UK
[3]Lead contact
*Correspondence: michael.tilby@bristol.ac.uk (M.J.T.), daniele.leonori@rwth-aachen.de (D.L.)
https://doi.org/10.1016/j.chempr.2025.102711

THE BIGGER PICTURE The hydrogenation of olefins is a fundamental transformation in both industry and academia. Traditional methods to achieve this process involve the use of hydrogen gas in combination with a transition metal catalysis. Although efficient, these protocols are associated with challenges, such as safety concerns, cost, and waste management, and they are often unselective. An idealized hydrogen-free and metal-free hydrogenation of olefins remains elusive. Herein, a metal-free photochemical hydrogenation of unactivated alkenes is reported employing ammonia-borane as a hydrogen surrogate. The method is reliant on amine-ligated boryl radical generation from a diaryl ketone photocatalyst, which then undergoes a complex series of radical transformation. Through a detailed mechanistic study, it is proposed that the steps include halogen-atom transfer with the solvent, *in situ* generation of alkyl borane intermediates, H-atom transfer to generate a borane-ligated aminyl radical, and subsequent β-fragmentation, all of which are turned over by a thiol co-catalyst. Overall, this reaction enables a mild, hydrogen-free, and metal-free hydrogenation of olefins tolerating functional groups typically incompatible with standard methods.

SUMMARY

Alkene hydrogenation is one of the most widely used reactions for producing high-value materials. Traditional methods rely on H_2 gas under transition metal catalysis, which presents challenges related to cost, safety, waste management, and undesired reactivity. An ideal hydrogenation method would circumvent both components by employing a hydrogen storage material under mild, metal-free conditions. Herein, we introduce a photocatalytic strategy for alkene hydrogenation using H_3N-BH_3. Our system harnesses visible light with a diaryl ketone photocatalyst to convert H_3N-BH_3 into its corresponding boryl radical. This open-shell species undergoes a complex sequence of transformations, including a key halogen-atom transfer with the solvent, *in situ* generation of alkyl borane intermediates, H-atom transfer to generate an aminyl radical, and subsequent β-fragmentation to engage with a thiol co-catalyst. This H_2- and metal-free approach enables the transformation of a broad range of alkenes, tolerating functional groups typically incompatible with standard protocols.

INTRODUCTION

Alkene hydrogenation is a fundamental transformation widely used in both academia and industry.[1–3] Given the abundance and efficiency of synthetic methods for olefin preparation,[4–6] hydrogenation strategies are essential for producing high-value materials such as pharmaceuticals and agrochemicals.[7] Indeed, it has been estimated that over 25% of all chemical transformations in the chemical industry involve hydrogenation at some stage.[8–10] As industries face increasing pressure to adopt more sustainable and energy-efficient processes,[11–13] developing catalytic hydrogenation methodologies is of paramount importance.

The direct addition of molecular hydrogen (H_2) to C=C π-systems remains the most effective hydrogenation approach, requiring the cleavage of the strong H–H σ-bond. Consequently, this transformation predominantly relies on precious transition metal catalysts such as Pd, Pt, Ir, and Rh (Figure 1A).[1–3] However, the extensive use of these metals has led to supply limitations and escalating costs.[14] Moreover, industrial-scale hydrogenations necessitate rigorous purification processes to remove trace metal contaminants, generating additional waste and disposal challenges.[15–17]

To reduce reliance on precious metals, significant efforts have been devoted to the development of hydrogenation methods

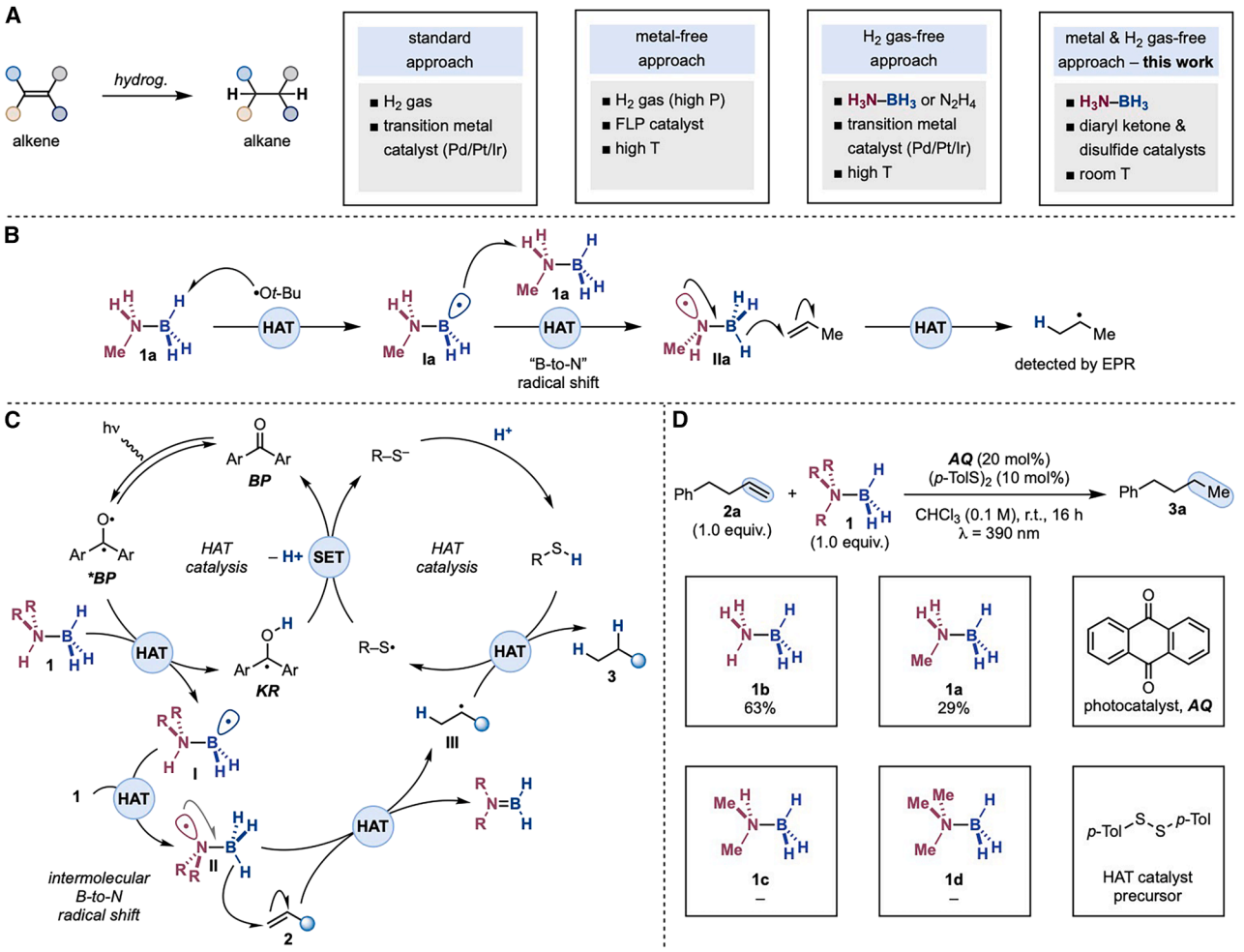

Figure 1. Alkene hydrogenation usually requires H_2 gas and metal catalysts, whereas this work provides a H_2-free and metal-free alternative using photocatalysis

(A) General approaches for alkene hydrogenation.

(B) EPR experiments from Roberts demonstrating HAT on alkenes via amine-ligated boryl radical **Ia**.

(C) Proposed catalytic mechanism for alkene hydrogenation using amine-boranes.

(D) Optimized reaction conditions for the hydrogenation of **2a** using an amine-borane reagent (see also Tables S1–S5 and S7–S9).

using earth-abundant transition metals (Co, Mn, and Fe),[18–20] alkali metals (K, Mg, and Ca),[21,22] and main-group elements (Ga, Ge, Bi, B, Si, and P).[23–25] Additionally, metal-free activation of H_2 has been achieved through the groundbreaking discovery of frustrated Lewis pair (FLP) catalysis.[26–28] Despite their innovation, FLP-mediated hydrogenations often require high temperatures ($T > 100°C$), high H_2 pressures, and strictly inert, anhydrous conditions (e.g., glove box setup). Moreover, FLP-based methods frequently struggle with substrates bearing polar functionalities.[29–32]

Although these alternative strategies address some limitations of conventional hydrogenation, challenges remain, particularly regarding the purification, storage, and safety of H_2 gas.[33–36] Notably, H_2 has a low gravimetric storage density (~1.5 wt %), meaning that a standard 300 mbar pressurized steel cylinder (~90 kg) holds a maximum of only 1.5 kg of H_2. Additionally, its low solubility[37] has driven extensive research into alternative hydrogen storage materials.[38,39] An ideal hydrogenation reagent would be a solid with high gravimetric hydrogen content, nonflammability, non-explosivity, and low toxicity, while enabling controlled H_2 release without the use of unsustainable metals.

Several methodologies have been developed to achieve the transfer of hydrogenation without molecular hydrogen, including the platinum-group-metal-catalyzed activation of water and alcohols.[40,41] Recently, an elegant photocatalytic method to activate water for radical hydrogenation with the aid of an iridium photocatalyst and a thiol co-catalyst has been reported.[42] Hydrazine has also been explored as a hydrogen surrogate,[43–46] though its inherent toxicity and frequent reliance on metal catalysis remain challenges.[47] An alternative approach involves metal-catalyzed hydrogen atom transfer (mHAT) reactions employing Mn, Co, and Fe.[48–50] These strategies build on the

Mukaiyama hydration reaction,[51] wherein a metal hydride acts as a hydrogen atom donor to an olefin. Productive catalysis often requires a silane reductant (e.g., $PhSiH_3$) and a stoichiometric oxidant such as a peroxide or fluoropyridinium species. More recently, Fe catalysis using alcoholic solvents and thiol co-catalysts[52] has enabled asymmetric hydrogenations, extending the scope of these methodologies.[53] Despite these advances, these approaches still rely on metals and energetic reducing agents, such as highly flammable liquid silanes (e.g., $PhSiH_3$).[54] This highlights the need for safer, more sustainable hydrogen storage materials.

Ammonia-borane (H_3N-BH_3), the coordination complex between Lewis-basic ammonia and Lewis-acidic borane, has emerged as a promising candidate due to its high gravimetric hydrogen content (~20 wt %), air stability, and non-toxicity.[55] Consequently, H_3N-BH_3 has been extensively studied as a hydrogen storage material.[56–60] Although H_3N-BH_3 has emerged as a promising hydrogen carrier, a number of limitations have hampered its use on an industrial scale. These limitations include the formation of complex polymeric mixtures after reaction and the difficulty of regeneration. Indeed, numerous works had been focused on the development of methods for efficient ammonia-borane regeneration; however, advances in this field are still needed to use it on large-scale operations.[61–65]

Hydrogen release from H_3N-BH_3 typically requires elevated temperatures (>90°C),[66,67] transition metal activation,[68–74] or, in a few cases, main-group element catalysis (P, Bi, and FLPs).[75–78] Although metal-free activation of H_3N-BH_3 under mild conditions has been achieved, its application has been largely restricted to activated π-bonds (e.g., C=N).[79–85] Given the current landscape of hydrogenation chemistry, there is a clear opportunity to exploit H_3N-BH_3 as a metal-free hydrogen surrogate capable of engaging unactivated olefins with diverse functional groups.

Herein, we present the development of a metal-free and H_2-free hydrogenation strategy that leverages diaryl ketone photocatalysis to convert stable H_3N-BH_3 into a reactive boryl radical intermediate. Hydrogenation of olefins is subsequently realized with the aid of a disulfide co-catalyst. As this strategy operates without transition metal catalysts or H_2 gas, it proceeds under mild, room-temperature conditions while tolerating a broad range of functional groups typically problematic under conventional hydrogenation protocols.

RESULTS AND DISCUSSION

Design plan

To harness amine-boranes as metal-free hydrogenation reagents, we drew inspiration from pioneering laser-flash photolysis (LFP) and electron paramagnetic resonance (EPR) studies from Roberts on the properties of their corresponding amine-ligated boryl radicals.[86,87] Various reports have documented that generating an electrophilic radical, such as *t*-BuO·, in the presence of amine-boranes (e.g. Et_3N-BH_3) triggers a kinetically favorable H-atom transfer (HAT) with the hydridic B–H bond (Figure 1B).[88] The resulting boryl radicals have been shown to participate efficiently in halogen-atom transfer (XAT) reactions with alkyl halides,[88,89] an approach that has recently been exploited in catalytic systems.[90–92]

However, for various amine-boranes such as MeH_2N-BH_3 (**1a**), which contains protic N–H bonds, EPR studies revealed the formation of the BH_3-ligated aminyl radical **IIa** upon HAT by *t*-BuO·.[93,94] Kinetic experiments rationalized that the initially generated amine-ligated boryl radical **Ia** rapidly undergoes intermolecular isomerization with a parent molecule (**1a**), forming the thermodynamically more stable aminyl radical **IIa**. Intriguingly, when these experiments were conducted in the presence of propene, the *i*-Pr radical was observed[95] instead of direct B-radical addition products.[96] Further D-labeling at boron experiments suggested that the transferred H-atom originated from the boron center.[94] This unexpected yet favorable isomerization to the aminyl radical effectively transforms the system into a [H·] donor, suggesting a potential platform for alkyl radical generation and subsequent HAT relay to achieve catalytic hydrogenation.

Based on these literature precedents, we envisioned a dual catalytic strategy for transition-metal-free and H_2-free alkene hydrogenation. As depicted in Figure 1C, we proposed a HAT/single-electron transfer (SET) photocatalytic cycle, wherein photoexcitation of a diaryl ketone (***BP***) catalyst enables conversion of an amine-borane reagent **1** into the corresponding boryl radical **I** via polarity-matched HAT.[88] A subsequent "B-to-N-radical shift" would afford the aminyl radical **II**, which serves as an [H·] donor for alkene (**2**) hydrogenation, generating the key alkyl radical **III**.[95] At this point, HAT between **III** and a thiol co-catalyst would furnish the hydrogenation product **3**, while generating a thyl radical capable of closing the photocatalytic cycle through SET and proton transfer with the ketyl radical, ***KR***.[97,98]

Reaction optimization

We initially observed that previous LFP experiments successfully engaged various alkene substitution patterns, with tetrasubstituted alkenes exhibiting the fastest reaction rates.[94] Based on this, we anticipated that monosubstituted alkenes would be more challenging. Therefore, we selected olefin **2a**, expecting it to enable a more general reaction framework (Figure 1D).

After evaluating all reaction parameters (Tables S1–S5, S8, and S9), we successfully employed the simplest amine-borane, H_3N-BH_3, in the reaction using anthraquinone (***AQ***) as the photocatalyst and $(p\text{-TolS})_2$ as the HAT catalyst. Under irradiation with purple light-emitting diodes (LEDs, λ = 390 nm) in $CHCl_3$ at room temperature, **2a** was hydrogenated to **3a** in 63% yield with just 1 equiv of H_3N-BH_3. The reaction demonstrated strong solvent specificity with high product formation exclusively in halogenated media (Tables S1, S9, and S10). Control experiments confirmed that the reaction proceeded via a photochemical pathway and did not occur in the absence of either catalyst (Table S7).

During reaction development, we found that the presence of protic N–H bonds in the amine-borane reagent was essential for reactivity (Table S8). However, increasing N-substitution (**1b** vs. **1a** vs. **1c** vs. **1d**) significantly reduced the product yield with no additional side products observed (Figure 1D). This result challenged our initial hypothesis, which assumed that increased methylation would weaken the N–H bond and favor isomerization and aminyl radical formation.

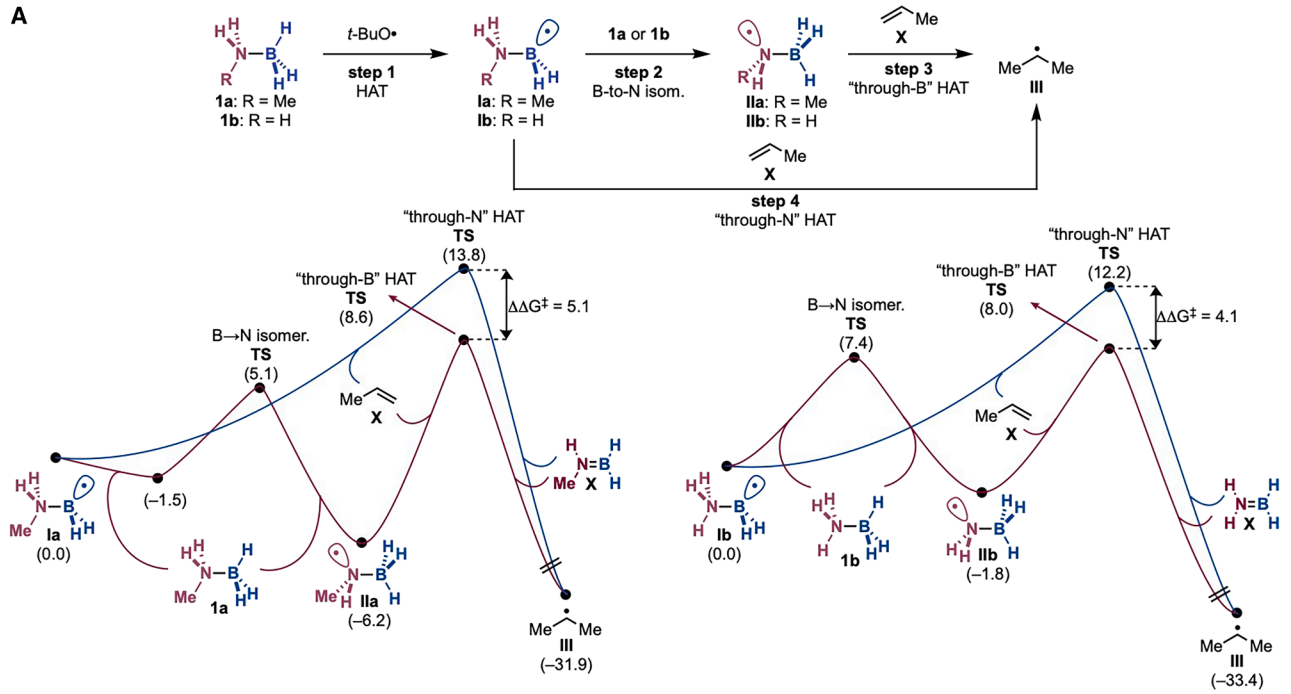

(legend on next page)

Mechanistic studies

To validate our reaction plan, we first computationally modeled the experimental results from Roberts (Tables S13–S15; Figures S38 and S39)[95] for the generation of the *i*-Pr radical from MeH_2N-BH_3 **1a** and propene under their experimentally relevant solvent 1,4-dioxane (see Section S11.4; Figures S40–S48). In agreement with their findings, HAT between **1a** and the electrophilic *t*-BuO· radical to generate the boryl radical **Ia** is kinetically favorable ($\Delta G^{\ddagger}$ = 10.4 kcal mol^{-1}) compared with aminyl radical generation ($\Delta G^{\ddagger}$ = 16.6 kcal mol^{-1}), albeit the aminyl radical **IIa** is the thermodynamic product (ΔG° = −6.2 kcal mol^{-1}, Figure S41). Due to the aminyl radical **IIa** being observed by EPR spectroscopy, we considered various reactions from the boryl radical (Figure 2A), including the "B-to-N isomerization" process (Figure S42), which revealed a low barrier intermolecular reaction with another molecule of **1a** ($\Delta G^{\ddagger}$ = 6.6 kcal mol^{-1}). Due to this feasible isomerization, there is the possibility for the reaction with both radicals **Ia** and **IIa** to react with propene via a "through-N" or "through-B" HAT. A significant kinetic penalty was observed for the through-N ($\Delta G^{\ddagger}$ = 13.8 kcal mol^{-1}) process. In comparison, the through-B reactivity was much more competitive ($\Delta\Delta G^{\ddagger}$ = 5.1 kcal mol^{-1}) and the most favorable process. This would support the initial EPR studies from Roberts[86] and also the potential design plan of isomerization and through-B H transfer.

Interestingly, modeling a similar reactivity framework for **1b** under analogous conditions revealed several significant differences (Figure 2A; see Section S11.5). Most notably, the amine-ligated boryl radical **Ib** and the borane-ligated aminyl radical **IIb** are closer to thermoneutral (ΔG° = −1.8 kcal mol^{-1}), with an increased barrier for B-to-N isomerization (step 3; $\Delta G^{\ddagger}$ = 7.4 kcal mol^{-1}). These results suggest a slower intermolecular isomerization, which agrees with EPR studies on **1b**, which detected **Ib** rather than **IIb**.[93] Regarding reactivity with propene, the through-B HAT from **IIb** remains facile (step 3; $\Delta G^{\ddagger}$ = 9.8 kcal mol^{-1}/ΔG_{TS} = 8.0 kcal mol^{-1} relative to **Ib**), whereas direct through-N HAT is still less favorable (step 4; $\Delta G^{\ddagger}$ = 12.2 kcal mol^{-1}).

Further mechanistic questions were raised by experimental results with deuterated amine-borane reagents, which revealed inconsistencies (Figure 2B; see Section S9.7; Figures S3–S28). From our density functional theory (DFT) calculations (Figure S47), it can be inferred that reactions with D_3N-BH_3 or H_3N-BD_3 should lead to extensive D/H scrambling during the B-to-N isomerization, leading to stochastic deuterium incorporation at both the internal and external positions of the alkene. However, when H_3N-BD_3 (85% D) was used, the deuterium appeared to selectively translocate to the internal position, with low labeling at the terminal position. In contrast, D_3N-BH_3 (97% D) resulted in effectively no internal deuteration and appreciable terminal labeling. Although, the deuterium at the external position appeared stochastic, these deuterium experiments directly challenged our initial mechanistic design, and we therefore questioned whether these results were more consistent with a through-N HAT process, without any isomerization occurring.

As our calculations indicated this pathway was kinetically uncompetitive, we speculated that quantum mechanical tunneling (QMT) could be lowering the effective barriers.[99–101] Extensive mechanistic analysis (detailed in the Sections S11.2 and S11.6; Figures S53–S62; Tables S16–S18) confirmed that **Ib** undergoes through-B and through-N HAT in fundamentally different manners. In particular, the through-N pathway shows significant conformational effects (Figure S51) and a complex potential energy surface for the lowest energy transition state conformer (Figure S57). However, when approximating the QMT contribution using canonical variational transition state theory and small-curvature tunneling (CVT/SCT), although significant, the phenomenological barrier remained too high to alter our overall kinetic conclusions. Furthermore, given the significance of QMT in the through-N pathway, a reaction using D_3N-BH_3 and proceeding through this mechanism should produce a kinetic isotope effect (KIE) greater than 7, whereas an experimental KIE of 2.19 was observed (based on the rate of the consumption of olefin), which ruled out QMT facilitating the through-N mechanism (Section S9.8; Figures S29–S32).

Although reevaluating the computation with a $CHCl_3$ implicit solvent model perturbed several barriers, it did not provide a satisfactory explanation for the deuterium results (Figures S49–S52; Table S17), which seemed to indicate control of selectivity at the internal position. Therefore, to clarify the reaction mechanism, we reevaluated several key experimental observations from the reaction development. Notably, the reaction exhibits a strong solvent specificity for halogenated media (Figure 2C; Table S9). In $CHCl_3$, crude reaction analysis consistently detected CH_2Cl_2 formation (Figure S29).[102] This suggests the involvement of a XAT process[88,90–92] between **Ib** and $CHCl_3$. Computational studies confirmed that this step is highly favorable ($\Delta G^{\ddagger}$ = 6.5 kcal $mol^{-=}$) and irreversible (ΔG° = −44.7 kcal mol^{-4}, Figure S63; Tables S19 and S20). This led us to consider the possible presence and role of chlorinated amine-borane species, rather than pure H_3N-BH_3, in the reaction mechanism (Table S11).

To reconcile the observed deuterium incorporation patterns, we hypothesized that *in situ* photocatalytic generation of H_3N-BH_2Cl or H_3N-$BHCl_2$ (**IV** or **V**, Figures S33 and S34) might react with the alkene via either a radical boryl radical addition

Figure 2. Mechanistic studies on the photocatalytic hydrogenation of alkenes using ammonia-borane

(A) Computational analysis of the elementary reactivity of amine-boranes **1a** and **1b** with prop-1-ene. DFT: SMD-(1,4-dioxane)-DSD-PBEB95-D3BJ/def2-QZVPP//SMD(1,4-dioxane)-M06-2X/def2-TZVP (see also Scheme S2).

(B) Deuterium labeling and kinetic isotope effect studies on the model substrate.

(C) Analysis of the solvent specificity and subsequent identification of halogen atom transfer reactivity (XAT).

(D) A proposed reaction channel leading to the hydrogenation products.

(E) Conversion of alkyl-boryl intermediates in a Brown oxidation.

(F) Application of hypothetical intermediates in the model reaction to establish hydrogen atom transfer (HAT) and fragmentation pathway. DFT: SMD-($CHCl_3$)-DSD-PBEB95-D3BJ/def2-QZVPP//SMD($CHCl_3$)-M06-2X/def2-TZVP.

(Figures S51 and S52)[103] or an ionic hydroboration pathway (Figure S66),[104] ultimately converging on an alkyl borane intermediate **VI** (see Section S9.9). Supporting this hypothesis, ^{1}H NMR time course monitoring in $CHCl_3$ (with d_3-MeCN aliquots) revealed that alkene consumption and product formation do not proceed concurrently but rather through transient intermediates (Figure S29). Though not isolable, these intermediates were tentatively assigned as B-alkylated ammonia-boranes through their chemical shifts, which are lower than the terminal methyl peak of **3a** (<0.8 ppm in $CDCl_3$ Figure S36) and have a characteristic multiplet at 0.01 ppm.

To experimentally validate the involvement of alkyl amine-boranes as precursors for the hydrogenated products, we applied a Brown oxidation ($NaOH/H_2O_2$) before reaction completion, yielding the corresponding alcohol **4** in high conversion (Figures 2E and S35).

However, this evidence raised the question of how the borylated intermediate is ultimately converted into the hydrogenation product.[105–108] An ionic protodeboronation pathway seemed unlikely; instead, a radical mechanism would be supported by the observation that a cyclopropyl-containing olefin (a radical probe) underwent ring opening (Figure S2; see also Scheme S1). We propose that various radical species, collectively denoted as [X·], can facilitate HAT from the N–H bond of reagent **VI** to give the borane-ligated aminyl radical **VII**. Based on the enthalpic and polar effects, we believe that the $Cl_2HC\cdot$ as well as **Ib** and the alkyl radicals **III** might be competent ($\Delta G^{\ddagger}$ = 13.3–27.8 kcal mol$^{-=}$, Figures S67 and S68) at this abstraction, thus leading to productive radical chain propagations. Species **IX** may then undergo β-fragmentation, generating an alkyl radical (**III**) that eventually leads to the desired product (**3**). Interestingly, the β-fragmentation step was determined by our computational studies to either occur concurrently with the HAT process or to be barrierless (Figure S50). As this type of photochemical radical process has not been previously identified in amine-borane chemistry, we sought to gather additional supporting evidence.

To test this mechanistic hypothesis, we prepared an alkyl ammonia-borane intermediate via an alternative thermal route (**5**, Figure 2F).[109] Though unstable and non-isolable, this species could be telescoped into the reaction, affording the hydrogenation product **3a** in analogous yields to the optimized procedure (59%). Additionally, control experiments demonstrated that without light, only decomposition occurred, whereas irradiation with either the disulfide or ***AQ*** alone still led to product formation (Table S12). This indicates that species such as **VI** are susceptible to HAT and subsequent β-scission, driving hydrogenation. Further support came from species **6**,[110] which lacks the N–H bonds necessary for HAT and was unreactive under our hydrogenation conditions (Figure S37).

In summary, although direct HAT activation of olefins using $H_3N\text{-}BH_3$ is plausible, our evidence points to a more complex pathway involving: (1) photocatalytic B-chlorination, generating chlorinated ammonia-borane species; (2) *in situ* olefin hydroboration, forming B-alkyl ammonia-borane intermediates; and (3) N–H bond-mediated radical deboronation via HAT and β-fragmentation. This mechanistic complexity highlights new dimension of amine-borane chemistry in this transformation.

Scope of the process

Given the complexity of the mechanism, we wanted to ensure that the method still provided a viable metal-free hydrogenation, tangential to other catalytic procedures. First, we evaluated the hydrogenation ability of our method across a series of terminal olefins containing different functional groups commonly used in organic synthesis (Figure 3). This scope exploration demonstrated tolerance of both enthalpically (**2b**, benzylic and allylic C(sp^3)-H) and kinetically (**2c–2g**, α-O-C(sp^3)-H) HAT-labile positions as well as several types of O-functionalities like free and silyl protected alcohol (**2c** and **2d**), ester (**2e** and **2f**), and mesylate (**2g**). Substrate **2h** contains a benzyl protected alcohol and therefore demonstrates the synthetic complementarity that our approach can provide over standard hydrogenation methods.[111,112] Indeed, although reduction using Pd/C and H_2 resulted in olefin hydrogenation and O-Bn deprotection (**3h′**), our method cleanly and selectively provided **3h**, leaving untouched the ether functionality. This transformation was also run on a gram-scale without significant variation of reaction yield (Section S6; Figure S1).

Nitrogen-based functionalities were evaluated next, and the method tolerated an alkylated indole (**2i**), known to undergo C2-C3 reduction with amine-boranes under thermal conditions,[113] as well as *N*-phthalimide (**2j**), nitro (**2k**), and sulfonamide (**2l**) groups. The ability of this method to react with olefin over other hydrogenation-sensitive functionalities was further demonstrated by the selective conversion of azide **2m** and *N*-Cbz protected piperidine **2n** into **3m** and **3n** without formation of **3m′** and **3n′**, which instead arose under standard Pd/C-based hydrogenations. Other functionalities that were tolerated included *N*-Boc protected amine (**2o**), ester (**2p**), nitrile (**2q**), amide (**2r**), alkyl bromide (**2s**), and isothiocyanate (**2t**). The compatibility with C(sp^3)–Br bonds (**2s**) is noteworthy because boryl radicals are excellent XAT mediators.[88,90–92]

We then tested the chemistry on terminal olefins installed across complex derivatives. These included the lactone containing (−)-camphanic acid (**2u**), the non-steroidal anti-inflammatory (NSAID) ibuprofen (**2v**), the HIV medicine nevirapine (**2w**), a glucofuranose (**2x**), and a complex bicyclic aminoalcohol derivative (**2y**). Pleasingly, in all cases, the desired products were obtained in good to high yields with full tolerance of the many functionalities present.

Having broadly determined the functional group compatibility of the process, we tested the hydrogenation across other classes of alkenes. In general, methods based on radical transfer hydrogenation reactivity can struggle to engage substituted olefins, so we were keen to determine whether our method could address such a limitation.[114,115] *gem*-disubstituted substrates were evaluated first and they were found compatible (**2z** and **2aa**), albeit the substituted 6-membered ring scaffold resulted in mixtures of *syn*- and *anti*-diastereomers. Pleasingly, this chemistry was also extended to the monoterpene (+)-limonene oxide that features an epoxide functionality (**2ab**). Also, in this case it is worth highlighting that transfer hydrogenation protocols based on the use of amine-boranes and transition metal catalysis result in epoxide cleavage, something that we can avoid under our conditions.[116]

Disubstituted olefins worked well in both acyclic (**2ac** and **2ad**) and cyclic systems (**2ae** and **2af**), also confirming that

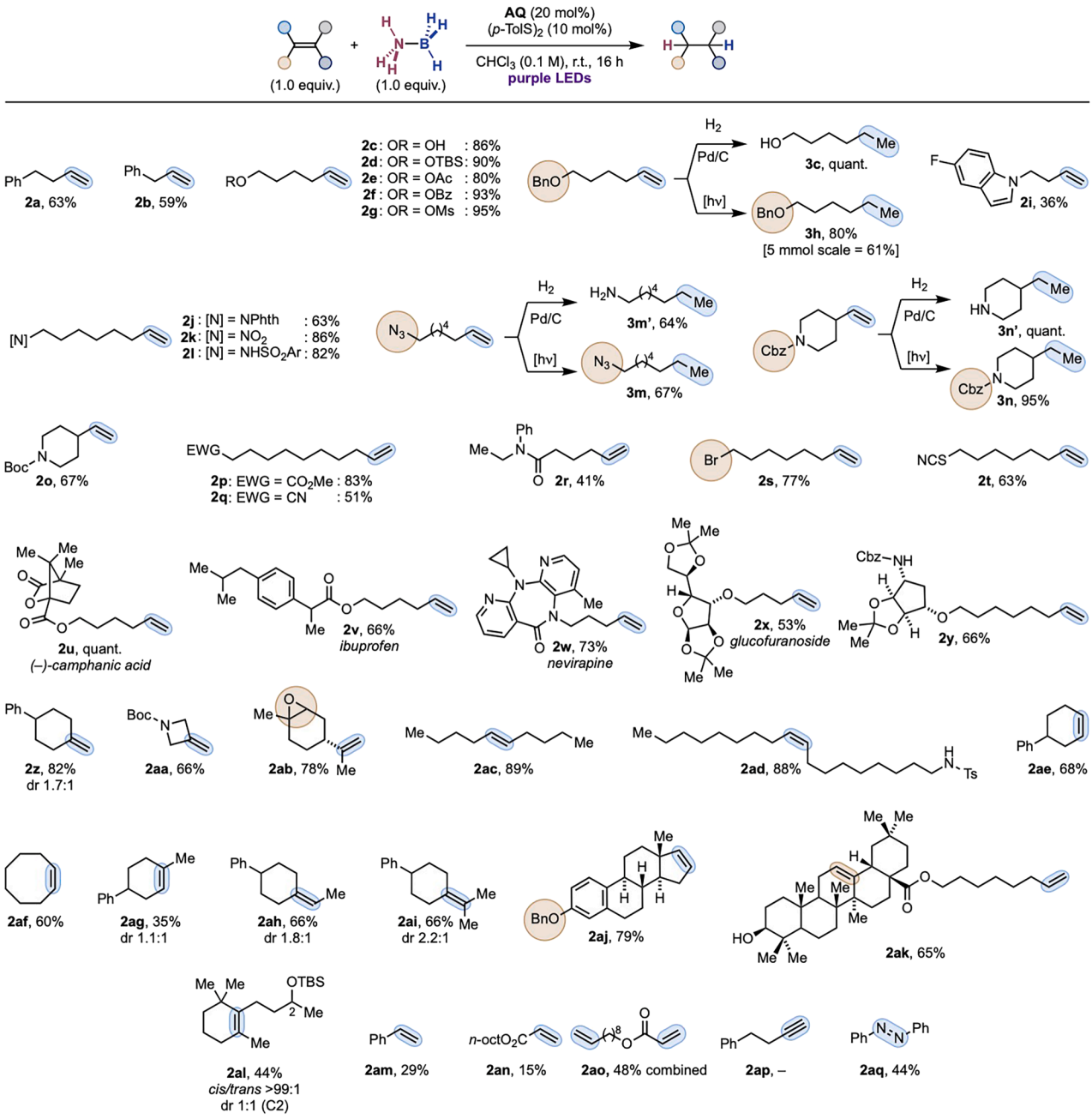

Figure 3. Scope of the metal-free and hydrogen-free hydrogenation process

The reaction on **2aq** was conducted at 80°C with 2.0 equiv of NH_3BH_3. Ar = 4-Cl-C_6H_4 (see also Table S6). "dr" refers to the diastereomeric ratio.

both *E* and *Z* isomers can be hydrogenated with equal efficiency. Moderate to good chemical yields were obtained for the reduction of tri- and tetrasubstituted derivatives (**2ag**–**2ai**). To the best of our knowledge, this class of materials can display limited reactivity in the application of boryl radical chemistry.[92] As a final element of substrate evaluation, we demonstrated high reactivity for the hydrogenation of an OBn-protected neurosteroid (**2aj**) and a functionalized oleanolic acid derivative (**2ak**). This last example features two chemically distinct olefins, and our method enabled selective targeting of the less sterically hindered one.

Tetrasubstituted endocyclic alkenes represent an interesting class of compounds, as their hydrogenation can yield different stereochemical outcomes depending on the underlying reaction mechanism. Notably, the hydrogenation of compound **2al**, prepared in two steps from dihydro-β-ionone, proceeded efficiently to furnish the *syn*-diastereomers (dr 1:1), consistent with the stereochemical outcome observed in Pd/C-catalyzed processes.

Regarding limitations (Section S8; Table S6), we observed poor reactivity with styrene (**2am**) and acrylate (**2an**) derivatives. Although the hydrogenation products were accessible, the reactions generated significant tarring, suggesting polymerization and potential addition of thiol to the alkene. Terminal alkene-containing acrylate **2ao** was hydrogenated with mild selectivity for the terminal olefin, delivering the acrylate-containing and fully hydrogenated products in a 1.7:1 ratio. Attempts to engage alkynes such as **2ap** resulted in full consumption of the starting material, but the hydrogenation products were not detected.

Finally, we demonstrated the utility of this approach for the hydrogenation of *E*-azobenzene (**2aq**). This reaction required increased equivalents of the ammonia-borane and a higher temperature (80°C), but control experiments confirmed the necessity of photochemical irradiation for successful conversion.

Conclusions

H_3N-BH_3 is a safe, non-toxic material of significant interest for hydrogen storage applications. However, the fundamental question of how to effectively activate this molecule remains an active area of research. To date, activation has been achieved primarily through thermolysis or transition metal catalysis. In this work, we present an alternative approach in which H_3N-BH_3 is activated via the formation of an amine-ligated boryl radical, enabled by mild diaryl ketone-based photocatalysis. This strategy provides a transition-metal-free and H_2-free protocol for the broad hydrogenation of alkenes, demonstrating tolerance for polar functionalities—including those traditionally incompatible with standard hydrogenation methods. Our mechanistic study indicates a complex interplay of radical reactions operating from the starting amine-ligated boryl radicals and converging to the desired hydrogenation products. An important aspect that will need to be addressed in the future relies on the regeneration and reuse of H_3N-BH_3. Although we have been able to obtain preliminary evidence supporting its feasibility (for further details see Section S10), this still represents a challenge in the use of these reagents. We hope that this work will fuel the development of other reactivity for the use of other hydrogen-storage materials under mild and metal-free settings.

METHODS

Detailed methods can be found in the supplemental information.

RESOURCE AVAILABILITY

Lead contact

Further information and requests should be direct to and will be fulfilled by the lead contact, Daniele Leonori (daniele.leonori@rwth-aachen.de).

Materials availability

All reagents in this study are either commercially available or can be easily prepared as indicated in supplemental information.

Data and code availability

All data for the replication of this work are given in the supplemental information or can be obtained by the lead contact upon reasonable request. DFT-optimized structures are provided in a separate zip file.

ACKNOWLEDGMENTS

D.L. thanks the European Research Council for a grant (101086901). E.R.-C. acknowledges Xunta de Galicia for her postdoctoral fellowship (ED481B 2022-056). W.J.O. thanks the Marie Skłodowska-Curie Actions for a fellowship (101102820). Computational calculations were performed with computing resources granted by RWTH Aachen University under project RWTH1268 and computational facilities of the Advanced Computing Research Centre, University of Bristol (http://www.bris.ac.uk/acrc/).

AUTHOR CONTRIBUTIONS

M.J.T. and D.L. designed the process. E.R.-C. and W.J.O. performed all experiments. M.J.T. performed all computational studies. All authors analyzed the results and wrote the manuscript.

DECLARATION OF INTERESTS

The authors declare no competing interests.

SUPPLEMENTAL INFORMATION

Supplemental information can be found online at https://doi.org/10.1016/j.chempr.2025.102711.

Received: March 17, 2025
Revised: June 2, 2025
Accepted: July 29, 2025
Published: August 25, 2025

REFERENCES

1. Chen, B., Dingerdissen, U., Krauter, J.G.E., Lansink Rotgerink, H.G.J.L., Möbus, K., Ostgard, D.J., Panster, P., Riermeier, T.H., Seebald, S., Tacke, T., et al. (2005). New developments in hydrogenation catalysis particularly in synthesis of fine and intermediate chemicals. Appl. Catal. A *280*, 17–46. https://doi.org/10.1016/j.apcata.2004.08.025.
2. Stoffels, M.A., Klauck, F.J.R., Hamadi, T., Glorius, F., and Leker, J. (2020). Technology Trends of Catalysts in Hydrogenation Reactions: A Patent Landscape Analysis. Adv. Synth. Catal. *362*, 1258–1274. https://doi.org/10.1002/adsc.201901292.
3. Martin Lok, C.M. (2024). Trends in selective hydrogenation. Catal. Today *430*, 114512. https://doi.org/10.1016/j.cattod.2024.114512.
4. Bender, M. (2014). An Overview of Industrial Processes for the Production of Olefins – C4 Hydrocarbons. ChemBioEng Rev. *1*, 136–147. https://doi.org/10.1002/cben.201400016.
5. Amghizar, I., Vandewalle, L.A., Van Geem, K.M.V., and Marin, G.B. (2017). New Trends in Olefin Production. Engineering *3*, 171–178. https://doi.org/10.1016/J.ENG.2017.02.006.
6. Chernyak, S.A., Corda, M., Dath, J.-P., Ordomsky, V.V., and Khodakov, A.Y. (2022). Light olefin synthesis from a diversity of renewable and fossil feedstocks: state-of the-art and outlook. Chem. Soc. Rev. *51*, 7994–8044. https://doi.org/10.1039/d1cs01036k.
7. Furrer, T., Levis, M., Berger, B., Kandziora, M., and Zogg, A. (2023). New Scale-Up Technologies for Multipurpose Pharmaceutical Production Plants: Use Case of a Heterogeneous Hydrogenation Process. Org. Process Res. Dev. *27*, 1365–1376. https://doi.org/10.1021/acs.oprd.3c00124.
8. Zhang, L., Zhou, M., Wang, A., and Zhang, T. (2020). Selective Hydrogenation over Supported Metal Catalysts: From Nanoparticles to Single Atoms. Chem. Rev. *120*, 683–733. https://doi.org/10.1021/acs.chemrev.9b00230.
9. Guo, M., Zhang, M., Liu, R., Zhang, X., and Li, G. (2022). State-of-the-Art Advancements in Photocatalytic Hydrogenation: Reaction Mechanism and Recent Progress in Metal-Organic Framework (MOF)-Based

Catalysts. Adv. Sci. (Weinh) *9*, e2103361. https://doi.org/10.1002/advs.202103361.

10. Zhao, E., Zhang, W., Dong, L., Zbořil, R., and Chen, Z. (2023). Photocatalytic Transfer Hydrogenation Reactions Using Water as the Proton Source. ACS Catal. *13*, 7557–7567. https://doi.org/10.1021/acscatal.3c00326.
11. Bowker, M., DeBeer, S., Dummer, N.F., Hutchings, G.J., Scheffler, M., Schüth, F., Taylor, S.H., and Tüysüz, H. (2022). Advancing Critical Chemical Processes for a Sustainable Future: Challenges for Industry and the Max Planck–Cardiff Centre on the Fundamentals of Heterogeneous Catalysis (FUNCAT). Angew. Chem. Int. Ed. Engl. *61*, e202209016. https://doi.org/10.1002/anie.202209016.
12. Colberg, J., Hii, K.K.M., and Koenig, S.G. (2022). Importance of Green and Sustainable Chemistry in the Chemical Industry. ACS Sustain. Chem. Eng. *10*, 8239–8241. https://doi.org/10.1021/acssuschemeng.2c03306.
13. Lopez, G., Keiner, D., Fasihi, M., Koiranen, T., and Breyer, C. (2023). From fossil to green chemicals: sustainable pathways and new carbon feedstocks for the global chemical industry. Energy Environ. Sci. *16*, 2879–2909. https://doi.org/10.1039/D3EE00478C.
14. (2019). Price pressures on metals. Nat. Catal. *2*, 735. https://doi.org/10.1038/s41929-019-0359-7.
15. Kushwaha, P. (2021). Metallic Impurities in Pharmaceuticals: An Overview. Curr. Pharm. Anal. *17*, 960–968. https://doi.org/10.2174/1573412916999200711151147.
16. Economidou, M., Mistry, N., Wheelhouse, K.M.P., and Lindsay, D.M. (2023). Palladium Extraction Following Metal-Catalyzed Reactions: Recent Advances and Applications in the Pharmaceutical Industry. Org. Process Res. Dev. *27*, 1585–1615. https://doi.org/10.1021/acs.oprd.3c00210.
17. Chatzopoulou, M., Madden, K.S., Bromhead, L.J., Greaves, C., Cogswell, T.J., Da Silva Pinto, S.D.S., Galan, S.R.G., Georgiou, I., Kennedy, M.S., Kennett, A., et al. (2022). Pilot Study to Quantify Palladium Impurities in Lead-like Compounds Following Commonly Used Purification Techniques. ACS Med. Chem. Lett. *13*, 262–270. https://doi.org/10.1021/acsmedchemlett.1c00638.
18. Chirik, P.J., Engle, K.M., Simmons, E.M., and Wisniewski, S.R. (2023). Collaboration as a Key to Advance Capabilities for Earth-Abundant Metal Catalysis. Org. Process Res. Dev. *27*, 1160–1184. https://doi.org/10.1021/acs.oprd.3c00025.
19. Wang, Y., Wang, M., Li, Y., and Liu, Q. (2021). Homogeneous manganese-catalyzed hydrogenation and dehydrogenation reactions. Chem *7*, 1180–1223. https://doi.org/10.1016/j.chempr.2020.11.013.
20. Chirik, P.J. (2015). Iron- and Cobalt-Catalyzed Alkene Hydrogenation: Catalysis with Both Redox-Active and Strong Field Ligands. Acc. Chem. Res. *48*, 1687–1695. https://doi.org/10.1021/acs.accounts.5b00134.
21. Gentner, T.X., and Mulvey, R.E. (2021). Alkali-Metal Mediation: Diversity of Applications in Main-Group Organometallic Chemistry. Angew. Chem. Int. Ed. Engl. *60*, 9247–9262. https://doi.org/10.1002/anie.202010963.
22. Bauer, H., Alonso, M., Färber, C., Elsen, H., Pahl, J., Causero, A., Ballmann, G., De Proft, F.D., and Harder, S. (2018). Imine hydrogenation with simple alkaline earth metal catalysts. Nat. Catal. *1*, 40–47. https://doi.org/10.1038/s41929-017-0006-0.
23. Chu, T., and Nikonov, G.I. (2018). Oxidative Addition and Reductive Elimination at Main-Group Element Centers. Chem. Rev. *118*, 3608–3680. https://doi.org/10.1021/acs.chemrev.7b00572.
24. Yadav, S., Saha, S., and Sen, S.S. (2016). Compounds with Low-Valent p-Block Elements for Small Molecule Activation and Catalysis. ChemCatChem *8*, 486–501. https://doi.org/10.1002/cctc.201501015.
25. Bawari, D., Toami, D., Jaiswal, K., and Dobrovetsky, R. (2024). Hydrogen splitting at a single phosphorus centre and its use for hydrogenation. Nat. Chem. *16*, 1261–1266. https://doi.org/10.1038/s41557-024-01569-y.
26. Welch, G.C., San Juan, R.R.S., Masuda, J.D., and Stephan, D.W. (2006). Reversible, Metal-Free Hydrogen Activation. Science *314*, 1124–1126. https://doi.org/10.1126/science.1134230.
27. Li, N., and Zhang, W.X. (2020). Frustrated Lewis Pairs: Discovery and Overviews in Catalysis. Chin. J. Chem. *38*, 1360–1370. https://doi.org/10.1002/cjoc.202000027.
28. Stephan, D.W. (2016). The broadening reach of frustrated Lewis pair chemistry. Science *354*, aaf7229. https://doi.org/10.1126/science.aaf7229.
29. Inés, B., Palomas, D., Holle, S., Steinberg, S., Nicasio, J.A., and Alcarazo, M. (2012). Metal-Free Hydrogenation of Electron-Poor Allenes and Alkenes. Angew. Chem. Int. Ed. Engl. *51*, 12367–12369. https://doi.org/10.1002/anie.201205348.
30. Hounjet, L.J., Bannwarth, C., Garon, C.N., Caputo, C.B., Grimme, S., and Stephan, D.W. (2013). Combinations of Ethers and B(C6F5)3 Function as Hydrogenation Catalysts. Angew. Chem. Int. Ed. Engl. *52*, 7492–7495. https://doi.org/10.1002/anie.201303166.
31. Greb, L., Oña-Burgos, P., Schirmer, B., Grimme, S., Stephan, D.W., and Paradies, J. (2012). Metal-free Catalytic Olefin Hydrogenation: Low-Temperature H2 Activation by Frustrated Lewis Pairs. Angew. Chem. Int. Ed. Engl. *51*, 10164–10168. https://doi.org/10.1002/anie.201204007.
32. Greb, L., Daniliuc, C.G., Bergander, K., and Paradies, J. (2013). Functional-Group Tolerance in Frustrated Lewis Pairs: Hydrogenation of Nitroolefins and Acrylates. Angew. Chem. Int. Ed. Engl. *52*, 5876–5879. https://doi.org/10.1002/anie.201210175.
33. Chandra, T., and Zebrowski, J.P. (2016). Hazards associated with laboratory scale hydrogenations. J. Chem. Health Saf. *23*, 16–25. https://doi.org/10.1016/j.jchas.2015.10.019.
34. West, M., Al-Douri, A., Hartmann, K., Buttner, W., and Groth, K.M. (2022). Critical review and analysis of hydrogen safety data collection tools. Int. J. Hydrog. Energy *47*, 17845–17858. https://doi.org/10.1016/j.ijhydene.2022.03.244.
35. Usman, M.R. (2022). Hydrogen storage methods: Review and current status. Renew. Sustain. Energy Rev. *167*, 112743. https://doi.org/10.1016/j.rser.2022.112743.
36. Hashimoto, T., Asada, T., Ogoshi, S., and Hoshimoto, Y. (2022). Main group catalysis for H2 purification based on liquid organic hydrogen carriers. Sci. Adv. *8*, eade0189. https://doi.org/10.1126/sciadv.ade0189.
37. Brunner, E. (1985). Solubility of hydrogen in 10 organic solvents at 298.15, 323.15, and 373.15 K. J. Chem. Eng. Data *30*, 269–273. https://doi.org/10.1021/je00041a010.
38. Züttel, A. (2003). Materials for hydrogen storage. Mater. Today *6*, 24–33. https://doi.org/10.1016/S1369-7021(03)00922-2.
39. Jain, I.P., Jain, P., and Jain, A. (2010). Novel hydrogen storage materials: A review of lightweight complex hydrides. J. Alloys Compd. *503*, 303–339. https://doi.org/10.1016/j.jallcom.2010.04.250.
40. Wang, Y., Huang, Z., Leng, X., Zhu, H., Liu, G., and Huang, Z. (2018). Transfer Hydrogenation of Alkenes Using Ethanol Catalyzed by a NCP Pincer Iridium Complex: Scope and Mechanism. J. Am. Chem. Soc. *140*, 4417–4429. https://doi.org/10.1021/jacs.8b01038.
41. Cummings, S.P., Le, T.-N., Fernandez, G.E., Quiambao, L.G., and Stokes, B.J. (2016). Tetrahydroxydiboron-Mediated Palladium-Catalyzed Transfer Hydrogenation and Deuteriation of Alkenes and Alkynes Using Water as the Stoichiometric H or D Atom Donor. J. Am. Chem. Soc. *138*, 6107–6110. https://doi.org/10.1021/jacs.6b02132.
42. Zhang, J., Mück-Lichtenfeld, C., and Studer, A. (2023). Photocatalytic phosphine-mediated water activation for radical hydrogenation. Nature *619*, 506–513. https://doi.org/10.1038/s41586-023-06141-1.
43. Furst, A., Berlo, R.C., and Hooton, S. (1965). Hydrazine as a Reducing Agent for Organic Compounds (Catalytic Hydrazine Reductions). Chem. Rev. *65*, 51–68. https://doi.org/10.1021/cr60233a002.
44. Imada, Y., Iida, H., and Naota, T. (2005). Flavin-Catalyzed Generation of Diimide: An Environmentally Friendly Method for the Aerobic

Hydrogenation of Olefins. J. Am. Chem. Soc. *127*, 14544–14545. https://doi.org/10.1021/ja053976q.

45. Humblot, A., Chave, T., Amaniampong, P.N., Streiff, S., and Jérôme, F. (2022). Sonochemically-Induced Reduction of Alkenes to Alkanes with Ammonia. Angew. Chem. Int. Ed. Engl. *61*, e202212719. https://doi.org/10.1002/anie.202212719.
46. Russo, C., Leech, M.C., Walsh, J.M., Higham, J.I., Giannessi, L., Lambert, E., Kiaku, C., Poole, D.L., Mason, J., Goodall, C.A.I., et al. (2023). eHydrogenation: Hydrogen-free Electrochemical Hydrogenation. Angew. Chem. Int. Ed. Engl. *62*, e202309563. https://doi.org/10.1002/anie.202309563.
47. Niemeier, J.K., and Kjell, D.P. (2013). Hydrazine and Aqueous Hydrazine Solutions: Evaluating Safety in Chemical Processes. Org. Process Res. Dev. *17*, 1580–1590. https://doi.org/10.1021/op400120g.
48. Shevick, S.L., Wilson, C.V., Kotesova, S., Kim, D., Holland, P.L., and Shenvi, R.A. (2020). Catalytic hydrogen atom transfer to alkenes: a roadmap for metal hydrides and radicals. Chem. Sci. *11*, 12401–12422. https://doi.org/10.1039/d0sc04112b.
49. Green, S.A., Crossley, S.W.M., Matos, J.L.M., Vásquez-Céspedes, S., Shevick, S.L., and Shenvi, R.A. (2018). The High Chemofidelity of Metal-Catalyzed Hydrogen Atom Transfer. Acc. Chem. Res. *51*, 2628–2640. https://doi.org/10.1021/acs.accounts.8b00337.
50. Crossley, S.W.M., Obradors, C., Martinez, R.M., and Shenvi, R.A. (2016). Mn-, Fe-, and Co-Catalyzed Radical Hydrofunctionalizations of Olefins. Chem. Rev. *116*, 8912–9000. https://doi.org/10.1021/acs.chemrev.6b00334.
51. Inoki, S., Kato, K., Takai, T., Isayama, S., Yamada, T., and Mukaiyama, T. (1989). Bis(trifluoroacetylacetonato)cobalt(II) Catalyzed Oxidation-Reduction Hydration of Olefins Selective Formation of Alcohols from Olefins. Chem. Lett. *18*, 515–518. https://doi.org/10.1246/cl.1989.515.
52. Kattamuri, P.V., and West, J.G. (2020). Hydrogenation of Alkenes via Cooperative Hydrogen Atom Transfer. J. Am. Chem. Soc. *142*, 19316–19326. https://doi.org/10.1021/jacs.0c09544.
53. Buzsaki, S.R., Mason, S.M., Kattamuri, P.V., Serviano, J.M.I., Rodriguez, D.N., Wilson, C.V., Hood, D.M., Ellefsen, J.D., Lu, Y.-C., Kan, J., et al. (2024). Fe/Thiol Cooperative Hydrogen Atom Transfer Olefin Hydrogenation: Mechanistic Insights That Inform Enantioselective Catalysis. J. Am. Chem. Soc. *146*, 17296–17310. https://doi.org/10.1021/jacs.4c04047.
54. Pesti, J., and Larson, G.L. (2016). Tetramethyldisiloxane: A Practical Organosilane Reducing Agent. Org. Process Res. Dev. *20*, 1164–1181. https://doi.org/10.1021/acs.oprd.6b00124.
55. Stephens, F.H., Pons, V., and Tom Baker, R.T. (2007). Ammonia–borane: the hydrogen source par excellence? Dalton Trans., 2613–2626. https://doi.org/10.1039/b703053c.
56. Hamilton, C.W., Baker, R.T., Staubitz, A., and Manners, I. (2009). B–N compounds for chemical hydrogen storage. Chem. Soc. Rev. *38*, 279–293. https://doi.org/10.1039/b800312m.
57. Staubitz, A., Robertson, A.P.M., and Manners, I. (2010). Ammonia-Borane and Related Compounds as Dihydrogen Sources. Chem. Rev. *110*, 4079–4124. https://doi.org/10.1021/cr100088b.
58. Lau, S., Gasperini, D., and Webster, R.L. (2021). Amine–Boranes as Transfer Hydrogenation and Hydrogenation Reagents: A Mechanistic Perspective. Angew. Chem. Int. Ed. Engl. *60*, 14272–14294. https://doi.org/10.1002/anie.202010835.
59. Demirci, U.B. (2017). Ammonia borane, a material with exceptional properties for chemical hydrogen storage. Int. J. Hydrog. Energy *42*, 9978–10013. https://doi.org/10.1016/j.ijhydene.2017.01.154.
60. Li, H., Yao, Z., Wang, X., Zhu, Y., and Chen, Y. (2022). Review on Hydrogen Production from Catalytic Ammonia Borane Methanolysis: Advances and Perspectives. Energy Fuels *36*, 11745–11759. https://doi.org/10.1021/acs.energyfuels.2c02314.
61. Sutton, A.D., Burrell, A.K., Dixon, D.A., III, Garner, E.B., Gordon, J.C., Nakagawa, T., Ott, K.C., Robinson, J.P., and Vasiliu, M. (2011). Regeneration of Ammonia Borane Spent Fuel by Direct Reaction with Hydrazine and Liquid Ammonia. Science *331*, 1426–1429. https://doi.org/10.1126/science.1199003.
62. Reller, C., and Mertens, F.O.R.L. (2012). A Self-Contained Regeneration Scheme for Spent Ammonia Borane Based on the Catalytic Hydrodechlorination of BCl3. Angew. Chem. Int. Ed. Engl. *51*, 11731–11735. https://doi.org/10.1002/anie.201201134.
63. Hausdorf, S., Baitalow, F., Wolf, G., and Mertens, F.O.R.L. (2008). A procedure for the regeneration of ammonia borane from BNH-waste products. Int. J. Hydrog. Energy *33*, 608–614. https://doi.org/10.1016/j.ijhydene.2007.10.035.
64. Davis, B.L., Dixon, D.A., Garner, E.B., Gordon, J.C., Matus, M.H., Scott, B., and Stephens, F.H. (2009). Efficient Regeneration of Partially Spent Ammonia Borane Fuel. Angew. Chem. Int. Ed. Engl. *48*, 6812–6816. https://doi.org/10.1002/anie.200900680.
65. Reller, C., and Mertens, F. (2018). The Recycling of Spent Ammonia Borane with $HBr/AlBr_3$ and Other HX/AlX_3-Based Schemes. ChemPlusChem *83*, 1013–1020. https://doi.org/10.1002/cplu.201800347.
66. Hu, M.G., Geanangel, R.A., and Wendlandt, W.W. (1978). The thermal decomposition of ammonia borane. Thermochim. Acta *23*, 249–255. https://doi.org/10.1016/0040-6031(78)85066-7.
67. Demirci, U.B. (2021). Mechanistic insights into the thermal decomposition of ammonia borane, a material studied for chemical hydrogen storage. Inorg. Chem. Front. *8*, 1900–1930. https://doi.org/10.1039/D0QI01366H.
68. Yüksel Alpaydın, C., Gülbay, S.K., and Ozgur Colpan, C. (2020). A review on the catalysts used for hydrogen production from ammonia borane. Int. J. Hydrog. Energy *45*, 3414–3434. https://doi.org/10.1016/j.ijhydene.2019.02.181.
69. Liu, M., Zhou, L., Luo, X., Wan, C., and Xu, L. (2020). Recent Advances in Noble Metal Catalysts for Hydrogen Production from Ammonia Borane. Catalysts *10*, 788. https://doi.org/10.3390/catal10070788.
70. Maspero, A., Bardelli, F., Konidaris, K.F., Uboldi, M., Lucarelli, C., Schiaroli, N., and Vitillo, J.G. (2024). Unraveling Transfer Hydrogenation Mechanisms by Ammonia Borane to Alkenes over Self-Healing Copper Nanoparticles: The Complementary Role of N–H Bond, Surface, and Solvent. ACS Catal. *14*, 9594–9606. https://doi.org/10.1021/acscatal.4c02556.
71. Chowdhury, D., Gupta, K., Gamidi, R.K., Jindal, G., and Mukherjee, A. (2024). Unraveling the Metal–Ligand Cooperativity in a Phosphine-Free Mn(II)-Catalyzed Transfer Hydrogenation of Nitriles to Primary Amines and Dehydrogenation of Dimethylamine Borane. ACS Catal. *14*, 15777–15789. https://doi.org/10.1021/acscatal.4c04988.
72. Fu, S., Chen, N.-Y., Liu, X., Shao, Z., Luo, S.-P., and Liu, Q. (2016). Ligand-Controlled Cobalt-Catalyzed Transfer Hydrogenation of Alkynes: Stereodivergent Synthesis of Z- and E-Alkenes. J. Am. Chem. Soc. *138*, 8588–8594. https://doi.org/10.1021/jacs.6b04271.
73. Shao, Z., Fu, S., Wei, M., Zhou, S., and Liu, Q. (2016). Mild and Selective Cobalt-Catalyzed Chemodivergent Transfer Hydrogenation of Nitriles. Angew. Chem. Int. Ed. Engl. *55*, 14653–14657. https://doi.org/10.1002/anie.201608345.
74. Park, B.Y., Kim, Y.J., and Han, M.S. (2024). In Situ Generated Bimetallic Nanoparticle Catalysts for the Transfer Semihydrogenation of Azoarenes. ACS Sustainable Chem. Eng. *12*, 11274–11282. https://doi.org/10.1021/acssuschemeng.4c02854.
75. Wang, F., Planas, O., and Cornella, J. (2019). Bi(I)-Catalyzed Transfer-Hydrogenation with Ammonia-Borane. J. Am. Chem. Soc. *141*, 4235–4240. https://doi.org/10.1021/jacs.9b00594.
76. Mo, Z., Rit, A., Campos, J., Kolychev, E.L., and Aldridge, S. (2016). Catalytic B–N Dehydrogenation Using Frustrated Lewis Pairs: Evidence for a Chain-Growth Coupling Mechanism. J. Am. Chem. Soc. *138*, 3306–3309. https://doi.org/10.1021/jacs.6b01170.
77. Dunn, N.L., Ha, M., and Radosevich, A.T. (2012). Main Group Redox Catalysis: Reversible P^{III}/P^{V} Redox Cycling at a Phosphorus Platform.

J. Am. Chem. Soc. *134*, 11330–11333. https://doi.org/10.1021/ja302963p.

78. Li, S., Li, G., Meng, W., and Du, H. (2016). A Frustrated Lewis Pair Catalyzed Asymmetric Transfer Hydrogenation of Imines Using Ammonia Borane. J. Am. Chem. Soc. *138*, 12956–12962. https://doi.org/10.1021/jacs.6b07245.

79. Yang, X., Zhao, L., Fox, T., Wang, Z.X., and Berke, H. (2010). Transfer Hydrogenation of Imines with Ammonia–Borane: A Concerted Double-Hydrogen-Transfer Reaction. Angew. Chem. Int. Ed. Engl. *49*, 2058–2062. https://doi.org/10.1002/anie.200906302.

80. Yang, X., Fox, T., and Berke, H. (2011). Facile metal free regioselective transfer hydrogenation of polarized olefins with ammonia borane. Chem. Commun. (Camb) *47*, 2053–2055. https://doi.org/10.1039/c0cc03163a.

81. Robertson, A.P.M., Leitao, E.M., and Manners, I. (2011). Catalytic Redistribution and Polymerization of Diborazanes: Unexpected Observation of Metal-Free Hydrogen Transfer between Aminoboranes and Amine-Boranes. J. Am. Chem. Soc. *133*, 19322–19325. https://doi.org/10.1021/ja208752w.

82. Veeraraghavan Ramachandran, P.V., Gagare, P.D., Sakavuyi, K., and Clark, P. (2010). Reductive amination using ammonia borane. Tetrahedron Lett. *51*, 3167–3169. https://doi.org/10.1016/j.tetlet.2010.04.014.

83. Zhao, W., Zhang, Z., Feng, X., Yang, J., and Du, H. (2020). Asymmetric Transfer Hydrogenation of N-Unprotected Indoles with Ammonia Borane. Org. Lett. *22*, 5850–5854. https://doi.org/10.1021/acs.orglett.0c01930.

84. Zhao, W., Feng, X., Yang, J., and Du, H. (2019). Asymmetric transfer hydrogenations of β-N-substituted enamino esters with ammonia borane. Tetrahedron Lett. *60*, 1193–1196. https://doi.org/10.1016/j.tetlet.2019.03.060.

85. Zhou, Q., Meng, W., Yang, J., and Du, H. (2018). A Continuously Regenerable Chiral Ammonia Borane for Asymmetric Transfer Hydrogenations. Angew. Chem. Int. Ed. Engl. *57*, 12111–12115. https://doi.org/10.1002/anie.201806877.

86. Lalevée, J., Blanchard, N., Chany, A.C., Tehfe, M.A., Allonas, X., and Fouassier, J.P. (2009). Effect of Lewis base coordination on boryl radical reactivity: investigation using laser flash photolysis and kinetic ESR. J. Phys. Org. Chem. *22*, 986–993. https://doi.org/10.1002/poc.1549.

87. Capaldo, L., Noël, T., and Ravelli, D. (2022). Photocatalytic generation of ligated boryl radicals from tertiary amine-borane complexes: An emerging tool in organic synthesis. Chem. Catal. *2*, 957–966. https://doi.org/10.1016/j.checat.2022.03.005.

88. Baban, J.A., Marti, V.P.J., and Roberts, B.P. (1985). Ligated boryl radicals. Part 2. Electron spin resonance studies of trialkylamin–boryl radicals. J. Chem. Soc. Perkin Trans. 2, 1723–1733. https://doi.org/10.1039/P29850001723.

89. Marti, V.P.J., and Roberts, B.P. (1986). Homolytic reactions of ligated boranes. Part 5. Spin-trapping and other addition reactions of ligated boryl radicals. J. Chem. Soc. Perkin Trans. 2, 1613–1621. https://doi.org/10.1039/p29860001613.

90. Pillitteri, S., Walia, R., Van der Eycken, E.V.V., and Sharma, U.K. (2024). Hydroalkylation of styrenes enabled by boryl radical mediated halogen atom transfer. Chem. Sci. *15*, 8813–8819. https://doi.org/10.1039/d4sc01731e.

91. Wan, T., Capaldo, L., Ravelli, D., Vitullo, W., de Zwart, F.J., de Bruin, B., and Noël, T. (2023). Photoinduced Halogen-Atom Transfer by N-Heterocyclic Carbene-Ligated Boryl Radicals for C(sp3)-C(sp3) Bond Formation. J. Am. Chem. Soc. *145*, 991–999. https://doi.org/10.1021/jacs.2c10444.

92. Zhang, Z.-Q., Sang, Y.-Q., Wang, C.-Q., Dai, P., Xue, X.-S., Piper, J.L., Peng, Z.-H., Ma, J.-A., Zhang, F.-G., and Wu, J. (2022). Difluoromethylation of Unactivated Alkenes Using Freon-22 through Tertiary Amine-Borane-Triggered Halogen Atom Transfer. J. Am. Chem. Soc. *144*, 14288–14296. https://doi.org/10.1021/jacs.2c05356.

93. Green, I.G., and Roberts, B.P. (1986). Homolytic reactions of ligated boranes. Part 3. Electron spin resonance studies of radicals derived from dialkylamine–boranes. J. Chem. Soc. Perkin Trans. 2, 1597–1606. https://doi.org/10.1039/P29860001597.

94. Kirwan, J.N., and Roberts, B.P. (1989). Homolytic reactions of ligated boranes. Part 11. Electron spin resonance studies of radicals derived from primary amine–boranes. J. Chem. Soc. Perkin Trans. 2, 539–550. https://doi.org/10.1039/P29890000539.

95. Kirwan, J.N., and Roberts, B.P. (1988). Hydrogen atom transfer to alkenes from aminyl–borane radicals. J. Chem. Soc. Chem. Commun., 480–482. https://doi.org/10.1039/C39880000480.

96. Sheeller, B., and Ingold, K.U. (2001). Absolute rate constants for some reactions of the triethylamine-boryl radical and the borane radical anion. J. Chem. Soc. Perkin Trans. 2, 480–486. https://doi.org/10.1039/b009494n.

97. Margrey, K.A., and Nicewicz, D.A. (2016). A General Approach to Catalytic Alkene Anti-Markovnikov Hydrofunctionalization Reactions via Acridinium Photoredox Catalysis. Acc. Chem. Res. *49*, 1997–2006. https://doi.org/10.1021/acs.accounts.6b00304.

98. Cao, H., Tang, X., Tang, H., Yuan, Y., and Wu, J. (2021). Photoinduced intermolecular hydrogen atom transfer reactions in organic synthesis. Chem. Catal. *1*, 523–598. https://doi.org/10.1016/j.checat.2021.04.008.

99. Meisner, J., and Kästner, J. (2016). Atom Tunneling in Chemistry. Angew. Chem. Int. Ed. Engl. *55*, 5400–5413. https://doi.org/10.1002/anie.201511028.

100. McMahon, R.J. (2003). Chemistry. Chemical Reactions Involving Quantum Tunneling. Science *299*, 833–834. https://doi.org/10.1126/science.1080715.

101. Schreiner, P.R. (2020). Quantum Mechanical Tunneling Is Essential to Understanding Chemical Reactivity. Trends Chem. *2*, 980–989. https://doi.org/10.1016/j.trechm.2020.08.006.

102. Fulmer, G.R., Miller, A.J.M., Sherden, N.H., Gottlieb, H.E., Nudelman, A., Stoltz, B.M., Bercaw, J.E., and Goldberg, K.I. (2010). NMR Chemical Shifts of Trace Impurities: Common Laboratory Solvents, Organics, and Gases in Deuterated Solvents Relevant to the Organometallic Chemist. Organometallics *29*, 2176–2179. https://doi.org/10.1021/om100106e.

103. Phang, Y.L., Jin, J.-K., Zhang, F.-L., and Wang, Y.-F. (2024). Radical hydroboration for the synthesis of organoboron compounds. Chem. Commun. (Camb) *60*, 4275–4289. https://doi.org/10.1039/d4cc00398e.

104. Clay, J.M., and Vedejs, E. (2005). Hydroboration with Pyridine Borane at Room Temperature. J. Am. Chem. Soc. *127*, 5766–5767. https://doi.org/10.1021/ja043743j.

105. Villa, G., Povie, G., and Renaud, P. (2011). Radical Chain Reduction of Alkylboron Compounds with Catechols. J. Am. Chem. Soc. *133*, 5913–5920. https://doi.org/10.1021/ja110224d.

106. Wilson, O.R., and Magenau, A.J.D. (2018). Oxygen Tolerant and Room Temperature RAFT through Alkylborane Initiation. ACS Macro Lett. *7*, 370–375. https://doi.org/10.1021/acsmacrolett.8b00076.

107. Gilbert, A., Langowski, P., Delgado, M., Chabaud, L., Pucheault, M., and Paquin, J.-F. (2020). Amine–borane complex-initiated SF5Cl radical addition on alkenes and alkynes. Beilstein J. Org. Chem. *16*, 3069–3077. https://doi.org/10.3762/bjoc.16.256.

108. Liautard, V., Delgado, M., Colin, B., Chabaud, L., Michaud, G., and Pucheault, M. (2022). In situ generation of radical initiators using amine-borane complexes for carbohalogenation of alkenes. Chem. Commun. (Camb) *58*, 2124–2127. https://doi.org/10.1039/d1cc06390a.

109. Ramachandran, P.V., Drolet, M.P., and Kulkarni, A.S. (2016). A non-dissociative open-flask hydroboration with ammonia borane: ready synthesis of ammonia–trialkylboranes and aminodialkylboranes. Chem.

Commun. (Camb) *52*, 11897–11900. https://doi.org/10.1039/c6cc06151f.

110. Buettner, C.S., Stavagna, C., Tilby, M.J., Górski, B., Douglas, J.J., Yasukawa, N., and Leonori, D. (2024). Synthesis and Suzuki–Miyaura Cross-Coupling of Alkyl Amine-Boranes. A Boryl Radical-Enabled Strategy. J. Am. Chem. Soc. *146*, 24042–24052. https://doi.org/10.1021/jacs.4c07767.

111. Wuts, P.G.M. (2014). Protective Groups in Organic Synthesis, Fourth Edition (John Wiley & Sons, Inc).

112. Yamamoto, Y., Shimizu, E., Ban, K., Wada, Y., Mizusaki, T., Yoshimura, M., Takagi, Y., Sawama, Y., and Sajiki, H. (2020). Facile Hydrogenative Deprotection of N–Benzyl Groups Using a Mixed Catalyst of Palladium and Niobic Acid-on-Carbon. ACS Omega *5*, 2699–2709. https://doi.org/10.1021/acsomega.9b03226.

113. Elliott, A.J., and Guzik, H. (1982). Borane Reduction of indoles with secondary amine substituents in a 2,3-fused side-chain. Tetrahedron Lett. *23*, 1983–1984. https://doi.org/10.1016/S0040-4039(00)87239-1.

114. King, S.M., Ma, X., and Herzon, S.B. (2014). A Method for the Selective Hydrogenation of Alkenyl Halides to Alkyl Halides. J. Am. Chem. Soc. *136*, 6884–6887. https://doi.org/10.1021/ja502885c.

115. Sang, S., Unruh, T., Demeshko, S., Domenianni, L.I., van Leest, N.P., Marquetand, P., Schneck, F., Würtele, C., de Zwart, F.J., de Bruin, B., et al. (2021). Photo-Initiated Cobalt-Catalyzed Radical Olefin Hydrogenation. Chemistry *27*, 16978–16989. https://doi.org/10.1002/chem.202101705.

116. Liu, X., Longwitz, L., Spiegelberg, B., Tönjes, J., Beweries, T., and Werner, T. (2020). Erbium-Catalyzed Regioselective Isomerization–Cobalt-Catalyzed Transfer Hydrogenation Sequence for the Synthesis of Anti-Markovnikov Alcohols from Epoxides under Mild Conditions. ACS Catal. *10*, 13659–13667. https://doi.org/10.1021/acscatal.0c03294.